can be made. In addition, the fact that atomic trajectories can be followed on a microscopic level is an advantageous feature in coupling ionization theories which will necessarily include the kinetic energy of the particle and its temporal local atomic environment.

Chemical Applications of Extended X-ray Absorption Fine Structure (EXAFS) Spectroscopy

Boon-Keng Teo

Bell Laboratories, Murray Hill, New Jersey 07974

Received January 28, 1980

Extended X-ray absorption fine structure (EXAFS) refers to the sinusoidal variation of the X-ray absorption as a function of photon energy beyond an absorption edge. The absorption, expressed in terms of absorption coefficient (μ), can be measured by a monitoring of the attenuation of X-rays upon their passage through a material. When the photon energy (E) is tuned to the binding energy of some core level of an atom in the material, an abrupt increase in μ, known as the absorption edge, occurs. For isolated atoms, μ decreases monotonically as a function of E beyond the edge. For atoms either in a molecule or embedded in solid, liquid, or matrix, the variation of μ at energies above the edge displays a fine structure (EXAFS) caused by backscattering of the ejected photoelectron from neighboring atoms.

Although the extended fine structure has been known for a long time,[1] its structural content was not fully recognized until the recent work of Stern, Lytle, and Sayers.[2] In addition, the recent availability of synchrotron radiation has resulted in establishment of EXAFS as a practical structural tool.[3] This technique is especially valuable for structural analyses of chemical or biological systems where conventional diffraction methods are not applicable.[4]

Qualitatively, the probability that an X-ray photon will be absorbed by a core electron depends on both initial and final states of the electron. The initial state is the localized core level corresponding to the absorption edge. The final state is that of the ejected photoelectron which can be represented as an outgoing spherical wave originating from the X-ray absorbing atom (absorber). If the absorbing atom is surrounded by a neighboring atom, the outgoing photoelectron wave will be backscattered by the neighboring atom, thereby producing an incoming electron wave. The final state is then the sum of the outgoing and all the incoming waves, one per each neighboring atom (scatterer). It is the interference between the outgoing and the incoming waves that gives rise to the sinusoidal variation of μ vs. E known as EXAFS (cf. Figure 1).

The *frequency* of each EXAFS wave depends on the distance between the absorbing atom and the neighboring atom since the photoelectron wave must travel from the absorber to the scatterer and back. On the other hand, the *amplitude* depends upon the number and the backscattering power of the neighboring atom as well as on its bonding to and distance from the absorber (vide infra). From an analysis of the frequency and amplitude of each wave, one can determine the distance and the number of each type of atoms surrounding the absorber, respectively.

Structural determinations via EXAFS depend on the feasibility of resolving the data into individual waves corresponding to the different types of neighbors of the absorbing atom. This can be accomplished by either curve-fitting or Fourier transform techniques. Curve fitting involves a best fitting of the data with a sum of

(1) R. de L. Kronig, *Z. Phys.*, **70**, 317 (1931); **75**, 191, 468 (1932).

(2) (a) E. A. Stern, *Phys. Rev. B*, **10**, 3027 (1974); (b) E. A. Stern, D. E. Sayers, and F. W. Lytle, *ibid.*, **11**, 4836 (1975), and references cited therein.

(3) (a) B. M. Kincaid and P. Eisenberger, *Phys. Rev. Lett.*, **34**, 1361 (1975); (b) H. Winick and A. Bienenstock, *Annu. Rev. Nucl. Part Sci.*, **28**, 33 (1978); (c) I. Lindau and H. Winick, *J. Vac. Sci. Technol.*, **15**, 977 (1978); (d) R. E. Watson and M. L. Perlman, *Science* **199**, (1978); (e) B. W. Batterman and N. W. Ashcroft, *Science*, **206**, 157 (1979).

(4) The physics, materials, and biological aspects of EXAFS have been reviewed elsewhere by others; see, e.g., (a) E. A. Stern, *Contemp. Phys.*, **19**, 289 (1978); (b) P. Eisenberger and B. M. Kincaid, *Science*, **200**, 1441 (1978); (c) R. G. Shulman, P. Eisenberger, and B. M. Kincaid, *Annu. Rev. Biophys. Bioeng.*, **7**, 559 (1978); (d) D. R. Sandstrom and F. W. Lytle, *Annu. Rev. Phys. Chem.*, **30**, 215 (1979); (e) S. P. Cramer and K. O. Hodgson, *Prog. Inorg. Chem.*, **25**, 1 (1979); (f) T. M. Hayes, *J. Non-Cryst. Solids*, **31**, 57 (1978); (g) J. Wong in "Metallic Glasses", H. J. Guntherodt, Ed., Springer-Verlag, Berlin, 1980; (h) "Synchrotron Radiation Research", H. Winick and S. Doniach, Eds., Plenum Press, New York, 1980; (i) "EXAFS Spectroscopy", B. K. Teo and D. Joy, Eds., Plenum Press, New York, 1981.

Boon-Keng Teo was born in China in 1948. He received his B.Sc. degree from the Chinese University of Hong Kong and his Ph.D. from the University of Wisconsin at Madison. He then joined Bell Laboratories at Murray Hill in 1973. Besides EXAFS spectroscopy, his research interests include the synthesis and structural investigation of metal tetrathiolene complexes and polymers, inorganic liquid crystals and dyes, and anticancer platinum drugs.
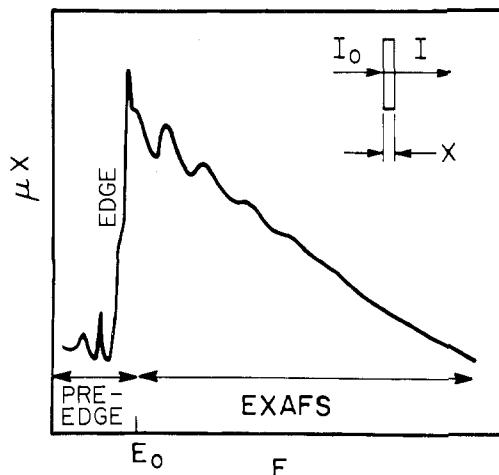
Figure 1. Schematic representation of the transmission experiment and the resulting X-ray absorption spectrum μx vs. E for an absorption edge of an absorber in a molecule (e.g., K edge of iron which corresponds to the ejection of a 1s electron by absorption of an X-ray photon with $E \geq E_0$, where E_0 is the threshold energy).

individual waves modeled by some empirical equations, each of which contains appropriate structural parameters for each type of neighbor. On the other hand, the Fourier transform technique provides a scattering profile as a function of the radial distance from the absorber. In such a radial distribution function, the positions of the peaks are related to the distances between the absorber and the neighboring atoms while the sizes of the peaks are related to the numbers and types of the neighboring atoms.

EXAFS differs from diffraction techniques in that, being mainly sensitive to short-range ordering,[5] it can focus on the immediate environment around each absorber (generally out to ~4 Å corresponding to 1–3 coordination shells). Other materials or impurities present in the sample which either do not contain the absorber or are far from the absorber will not interfere. Furthermore, it is highly versatile in that it can be applied with high accuracy (0.01~0.03 Å) to matter in the solid (crystalline or amorphous), liquid, solution, or gaseous state.

EXAFS Spectroscopy: Theory and Practice

EXAFS spectroscopy involves the measurement of the X-ray absorption coefficient μ as a function of photon energy E above the threshold of an absorption edge. Figure 1 shows schematically one edge of an absorber. In a transmission experiment, μ or μx (x is the sample thickness) is given by

$$\mu x = \ln I_0/I \qquad (1)$$

where I_0 and I are the intensities of the incident and transmitted beams, respectively. EXAFS spectra generally refer to the region 40–1000 eV above the ab-

sorption edge. In the pre-edge region (cf. Figure 1) there generally appear absorption peaks due to photoexcitation of electrons from the core level of the absorber to some discrete empty bound states. The edge energy also contains information about the charge on the absorber.[6]

Transmission is just one of several modes of EXAFS measurement. There is also the fluorescence technique which involves the measurement of the fluorescence radiation, integrated over a solid angle, at right angle to the incident beam.[7a-c] For dilute biological systems, this method removes the "background" absorption due to other constituents such as solvent, thereby providing greater sensitivity. Two additional methods include surface EXAFS (SEXAFS) which involve measurements in vacuum of either the Auger electrons produced when an atom that has absorbed a photon relaxes[7d] or a portion of the inelastically scattered electrons (partial electron yield,[7e] and electron energy loss (inelastic electron scattering) spectroscopy (EELS).[7f-j] These latter methods are useful for light atom EXAFS with edge energies up to a few kiloelectronvolts.

The simple picture of EXAFS has been formulated into a generally accepted *short-range single-electron single-scattering* theory[2,8] which assumes that the single photoelectron ejected from an absorbing atom makes a *single* round trip from the absorber to the nearby scatterers which lie within a *short distance* ($< \sim 4$ Å) *range* from the absorber. For reasonably high energy (≥ 60 eV) the fractional modulation (χ) of the total absorption coefficient (μ) as a function of the photon energy (E) is given by

$$\chi(E) = \frac{\mu(E) - \mu_0(E)}{\mu_0(E)} \qquad (2)$$

where μ_0 is the smooth "background" absorption coefficient.[9] In order to relate $\chi(E)$ to structural parameters, it is necessary to convert E into the photoelectron wavevector $\mathbf{k}$ by the relationship

$$\mathbf{k} = [2m(E - E_0)/\hbar^2]^{1/2} \qquad (3)$$

where E_0 is the threshold energy of the absorption edge. This transformation of $\chi(E)$ into $\chi(\mathbf{k})$ in $\mathbf{k}$ space gives rise to

$$\chi(\mathbf{k}) = \sum_j N_j F_j(\mathbf{k}) e^{-2\sigma_j^2 k^2} \frac{e^{-2r_j/\lambda}}{k r_j^2} \sin(2k r_j + \phi_j(\mathbf{k})) \qquad (4)$$

(5) For crystalline materials with long-range order, X-ray or neutron diffraction methods can provide a three-dimensional picture of atomic coordinates via a Fourier transformation of the measured diffracted intensities (Bragg's law). For materials with only short-range order (amorphous solid, liquid, or solution), X-ray scattering experiments provide only diffuse halos which, upon Fourier transformation, give rise to a one-dimensional radial distribution function (RDF). Such a RDF contains interatomic distances due to all atom pairs in the sample (condensed to one arbitrary origin). On the other hand, EXAFS measurements can provide structural information for each type of atoms by simply tuning the X-ray energy to coincide successively with an absorption edge of each of the atom types in the sample.

(6) (a) U. C. Srivastava and H. L. Nigam, *Coord. Chem. Rev.*, **9**, 275 (1972–73); (b) R. G. Shulman, Y. Yafet, P. Eisenberger, and W. E. Blumberg, *Proc. Natl. Acad. Sci. U.S.A.* **73**, 1384 (1976); (c) F. W. Lytle, P. S. P. Wei, R. B. Greegor, G. H. Via, and J. H. Sinfelt, *J. Chem. Phys.* **70**, 4849 (1979).

(7) (a) J. Jaklevic, J. A. Kirby, M. P. Klein, A. S. Robertson, G. S. Brown, and P. Eisenberger, *Solid State Commun.*, **23**, 679 (1977); (b) F. S. Goulding, J. M. Jaklevic, and A. C. Thompson, SSRL Report No. 78/04, May 1978; (c) E. A. Stern and S. M. Heald, *Rev. Sci. Instrum.*, **50**, 1579 (1979); (d) P. H. Citrin, P. Eisenberger, and R. Hewitt, *Phys. Rev. Lett.*, **41**, 309 (1978); (e) J. Stohr, D. Denley, P. Perfetti, *Phys. Rev. B*, **18**, 4132 (1978); (f) M. Isaacson, *J. Chem. Phys.*, **56**, 1818 (1972); (g) J. I. Ritsko, S. E. Schnatterly, and P. G. Gibbons, *Phys. Rev. Lett.*, **32**, 671 (1974); (h) R. A. Bonham in "Momentum Wave Functions-1976", American Institute of Physics, New York, 1977; (i) B. M. Kincaid, A. E. Meixner, and P. M. Platzman, *Phys. Rev. Lett.*, **40**, 1296 (1978); (j) D. C. Joy and D. M. Maher, *Science*, **206**, 162 (1979).

(8) (a) C. A. Ashley and S. Doniach, *Phys. Rev. B*, **11**, 1279 (1975); (b) P. A. Lee and G. Beni, *ibid.*, **15**, 2862 (1977).

(9) Though simply defined as $\chi = (\mu - \mu_0)/\mu_0$, the determination of χ from μ (generally termed as "background subtraction") is complicated by the fact that μ_0 is generally not known. A general procedure is to approximate μ_0 by a smooth curve (some polynomial or Spline) fitted to the experimentally determined μ.
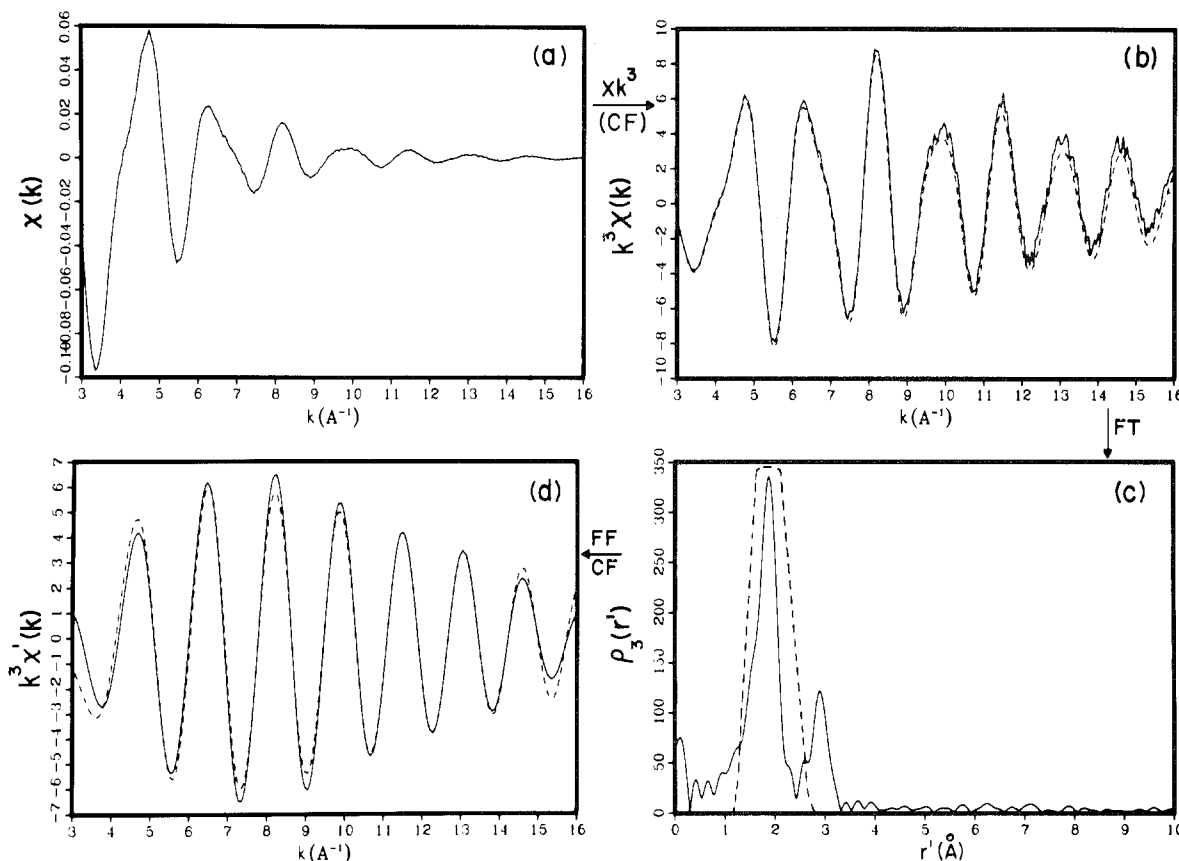
Figure 2. Data reduction and data analysis in EXAFS spectroscopy: (a) EXAFS spectrum $\chi(k)$ vs. k after background removal; (b) the solid curve is the weighted EXAFS spectrum $\chi(k)k^3$ vs. k after multiplying $\chi(k)$ by k^3. The dashed curve represents an attempt to fit the data with a two-distance model by curve-fitting (CF) technique; (c) Fourier transformation (FT) of the weighted EXAFS spectrum in momentum (k) space into the radial distribution function $\rho_3(r')$ vs. r' in distance space, r' is related to the true distance r by a "phase shift" $\alpha = r - r'$. The dashed curve is the window function used to filter the major peak in Fourier filtering (FF); (d) Fourier-filtered EXAFS spectrum $\chi'(k)k^3$ vs. k (solid curve) of the major peak in (c) after backtransforming into k space. The dashed curve attempts to fit the filtered data with a single-distance model.

where $F_j(k)$ is the backscattering amplitude[10] from each of the N_j neighboring atoms of type j, σ_j is the Debye-Waller factor which accounts for thermal vibration (assume harmonic) and possible static disorder, viz., distribution of distances (assume symmetric), and r_j is the distance of the jth atom from the absorber. The total phase shift experienced by the photoelectron is given by $\phi_j = \phi_a{}^l + \phi_b - l\pi$ ($l = 1$) for K or L_I and 2 for L_{II} or L_{III} edges where $\phi_a{}^l$ and ϕ_b are the phase shifts[10] due to the absorber and the jth scatterer, respectively. The term $e^{-2r_j/\lambda}$ is due to inelastic scattering losses with λ being the electron mean free path.

In order for EXAFS to provide accurate structural and chemical information, three assumptions must be made:[2,8,11] (1) EXAFS is a simple sum of waves due to various types of neighboring atoms (this implies that multiple scattering is relatively unimportant); (2) the amplitude function is transferable for each type of backscatterer B; and (3) the phase function is transferable for each pair of atoms A–B, where A is the absorber and B is the backscatterer. Transferability implies that these functions are relatively insensitive to chemical bonding for energies 60–1000 eV above the

absorption edge such that once determined for a known system, they can be applied to unknown systems which contain the same corresponding elements.

There are two major approaches to EXAFS data analysis: the Fourier transform (FT) and the curve fitting (CF) techniques. In either method, the μ vs. E data (Figure 1) is converted into $\chi(k)$ vs k via eq 2 and 3 (Figure 2a).[9] $\chi(k)$ is then multiplied by some power of k so as to compensate for the diminishing amplitudes at high k values to give $\chi(k)k^n$ for which a weighting scheme of $n = 3$ is commonly used (solid curve in Figure 2b).

The CF technique[11] attempts to best fit (e.g., by least-squares refinement) the $\chi(k)k^n$ spectra in k space with some empirical model based on eq 4 (dashed curve in Figure 2b). The FT method[2,8] corresponds to the Fourier inversion of $\chi(k)k^n$ in momentum (k) space to give the radial distribution function $\rho_n(r')$ in distance (r') space (Figure 2c). Each peak in $\rho_n(r')$ is shifted from the true distance r by $\alpha = r - r'$ where α amounts to ca 0.2~0.5 Å depending upon the elements involved. The FT approach has the advantage of providing a simple physical picture via the radial distribution function whereas the CF method can provide better resolution, especially for multidistance systems. A compromise of

(10) It should be emphasized that while the amplitude function $F(k)$ depends only on the type of scatterers (neighboring atoms), the phase function contains contributions (simple sums) from both the absorber and the scatterer. The reason is that, during the trip, the photoelectron experiences a phase shift (Coulombic interaction) of the absorber twice ($\phi_a = 2\delta'$), once going out and once coming back, and a phase shift of the scatterer once ($\phi_b = \theta$) upon scattering.[18]

(11) (a) P. H. Citrin, P. Eisenberger, and B. M. Kincaid, *Phys. Rev. Lett.*, **36**, 1346 (1976); (b) B. K. Teo, P. A. Lee, A. L. Simons, P. Eisenberger, and B. M. Kincaid, *J. Am. Chem. Soc.*, **99**, 3854 (1977); (c) P. A. Lee, B. K. Teo, and A. L. Simons, *ibid.*, **99**, 3856 (1977).

these two approaches is Fourier filtering (FF) followed by curve fitting. It involves Fourier transforming the $\chi(k)k^n$ data into the distance space, selecting the distance range of interest with some smooth window (dashed curve in Figure 2c), and transforming the data back to **k** space (Figure 2d). The resulting "filtered" EXAFS spectra $\chi'(k)k^n$ can then be fitted with simpler models (dashed curve in Figure 2d).[12]

Each EXAFS wave contains two sets of highly correlated variables: $\{F(k), \sigma, \lambda, N\}$ and $\{\phi(k), E_0, r\}$. Significant correlations can occur both *within* and *between* these two sets of variables as well as *between* different scattering terms. In order to determine N and σ, $F(k)$ must be known reasonable well; similarly, in order to determine r, $\phi(k)$ must be known accurately. While $F(k)$ and $\phi(k)$ can be determined empirically from model compounds, it is clearly desirable to calculate them from first principles. By use of an electron–atom scattering model,[8b] these functions, which vary systematically with atomic number, have been calculated for most elements in the periodic table (cf. Figure 3).[13] These theoretical functions[13] and their parameterized versions[11b,c] are widely used in EXAFS analyses with better than 0.5%, 10%, and 20% accuracy in r, σ, and N determinations, respectively.

The Debye–Waller factor σ plays an important role in EXAFS spectroscopy. It contains both structural data (i.e., nonequivalence in distances, σ_{stat})[14a] and chemical information (vibrational amplitude of the bonds, σ_{vib})[14b] such that, based upon assumed harmonic motion and Gaussian pair distribution,

$$\sigma^2 = \sigma_{stat}^2 + \sigma_{vib}^2 \qquad (5)$$

Separation of the effective σ into these two contributions usually requires a study of its temperature dependence since σ_{vib} is related to the vibrational frequency ν and temperature T. For systems with large σ ($\gtrsim 0.1$ Å) and/or anharmonic vibration and/or asymmetric pair distribution, a generalized EXAFS formulation must be used.[14c]

Most of recent EXAFS work are done using synchrotron radiation.[15a] These highly collimated, plane

(12) It should be mentioned that after FF, CF is not the only option. For single-scatterer peaks, a plot of $\ln(A(k)/A_s(k))$ vs. k^2 where $A(k)$ is the amplitude envelope gives rise to a linear curve with an intercept of $\ln(N/N_s \times r_s^2/r^2)$ and a slope of $2(\sigma_s^2 - \sigma^2)$.[2b] The subscript s denotes the model compound of known structure. For systems with a large disparity in distances, a beat-node technique may also be used (G. Martens, P. Rabe, N. Schwentner, and A. Werner, *Phys. Rev. Lett.*, **39**, 1411 (1977), and *Phys. Rev. B*, **17**, 1481 (1978)).

(13) B. K. Teo and P. A. Lee, *J. Am. Chem. Soc.*, **101**, 2815 (1979).

(14) (a) For a two-distance system with m bonds at a distance r_m and n bonds at a distance r_n, σ_{stat} reduces to

$$\sigma_{stat} \approx \frac{\sqrt{mn}}{m+n} |r_m - r_n| = \frac{\sqrt{mn}}{m+n} \Delta r$$

(b) Assuming harmonic motion, $\sigma^2_{vib} = (h/8\pi^2\mu\nu) \coth(h\nu/2kT)$, where μ is the reduced mass, T is the temperature, and ν is the vibrational frequency. See, for example, S. J. Cyvin, "Molecular Vibrations and Mean Square Amplitudes", Elsevier, Amsterdam, 1968, p 77. For detailed discussions on determination and calculation of EXAFS σ, see G. Beni and P. M. Platzman, *Phy. Rev. B*, **14**, 1514 (1976); R. B. Greegor and F. W. Lytle, *ibid.*, **20**, 4902 (1979); and E. Sevillano, H. Meuth, and J. J. Rehr, *ibid.*, **20**, 4908 (1979). (c) For systems with large anharmonicity in σ or large asymmetry in r (non-Gaussian pair distribution), an apparent contraction in distance and a significant reduction in amplitude may result which require a more general formulation of EXAFS. See, for example, G. Brown and P. Eisenberger, *Solid State Commun.*, **29**, 481 (1979), and T. M. Hayes, J. B. Boyce, and J. L. Beeby, *J. Phys. C*, **11**, 2931 (1978).

polarized, and precisely pulsed tunable intense X-rays, with fluxes of $10^{12} \sim 10^{16}$ photons s^{-1} $mrad^{-1}$ mA^{-1}, greatly improve the signal-to-noise ratio. The improvement can reach a factor of 10^6 over that obtainable from conventional sources.[15b]

It is important to choose an absorption edge of a particular absorber whose energy corresponds to the brightest synchrotron radiation in the spectral distribution as well as to minimal harmonics in the X-ray beam. Currently at SSRL, either the EXAFS I or Wiggler beam line covers an energy range of 3–35 keV, which includes K edges of elements from potassium to iodine and L edges of elements through the end of the periodic table. The focused beam line, which has approximately 100 times greater relative intensity, spans a 3–9-keV range, including K edges of elements from potassium to copper. The Wiggler line (using the Wiggler magnets) not only provides an X-ray intensity which is greater by a factor of $6 \sim 100$ than EXAFS I line (using bending magnets), but also increases the range of accessible X-ray energies by a factor of $2 \sim 10$.

A new source of high-intensity, nanosecond-pulsed *soft* X-rays ($\lesssim 3$ keV) has recently been generated from a laser-produced plasma.[15c] This technique is useful for EXAFS studies of low Z elements (K edge of the elements from carbon to sulfur and L edge of the elements from sulfur to molybdenum) which are at present difficult to study with other sources. It enables studies of transient species since an EXAFS spectrum can be recorded on film in a few nanoseconds with a *single pulse* of laser-produced X-rays.

The sample thickness or concentration depends on the total absorption coefficient of the material. Optimum signal-to-noise ratio occurs at $\mu x \approx 2$. For concentrations less than 10^{-3} M it may be necessary to use the fluorescence technique and/or to average over many spectra. For weak chemical bonds or large σ_{vib}, it may be useful to perform the measurements at lower temperatures.[14b]

Other factors of importance are as follows. First, K(1s) and L_I(2s) edges require the same set of amplitude and phase functions, whereas an $L_{II}(2p_{1/2})$ or $L_{III}(2p_{3/2})$ edge requires a different central atom phase shift (vide supra).[13] Second, the energy range above and below the edge must be >600 eV to prevent interference from adjacent edge(s). Third, the edge jump must be sizeable since EXAFS is a measure of the fractional oscillation of the absorption relative to the edge jump. Fourth, absorption or absorption edges due to other elements in the material should be minimized or avoided to prevent a sloping background or interference. Finally, at low energies, absorptions due to sample cells and intervening air may pose some difficulties. The former problem can be reduced by the use of X-ray transparent tapes as windows whereas the latter may require a helium path.

Application to Biochemical Systems

EXAFS can be used to probe the prosthetic group of a protein, thereby allowing structure–function correla-

(15) (a) Synchrotron radiation in the UV and X-ray regions is available at SSRL (Stanford), CHESS (Cornell), Tantalus I (Wisconsin), and SURF II (NBS) in the U.S. as well as DESY (Germany), ARUS (USSR), BONN (Germany), INS-SOR II (Japan), Frascati (Italy),NINA (England), DCI (France), etc. (b) G. S. Knapp, H. Chen, T. E. Klippert, *Rev. Sci. Instrum.*, **49**, 1658 (1978); (c) P. J. Mallozzi, R. E. Schwerzel, H. M. Epstein, and B. E. Campbell, *Science*, **206**, 353 (1979).
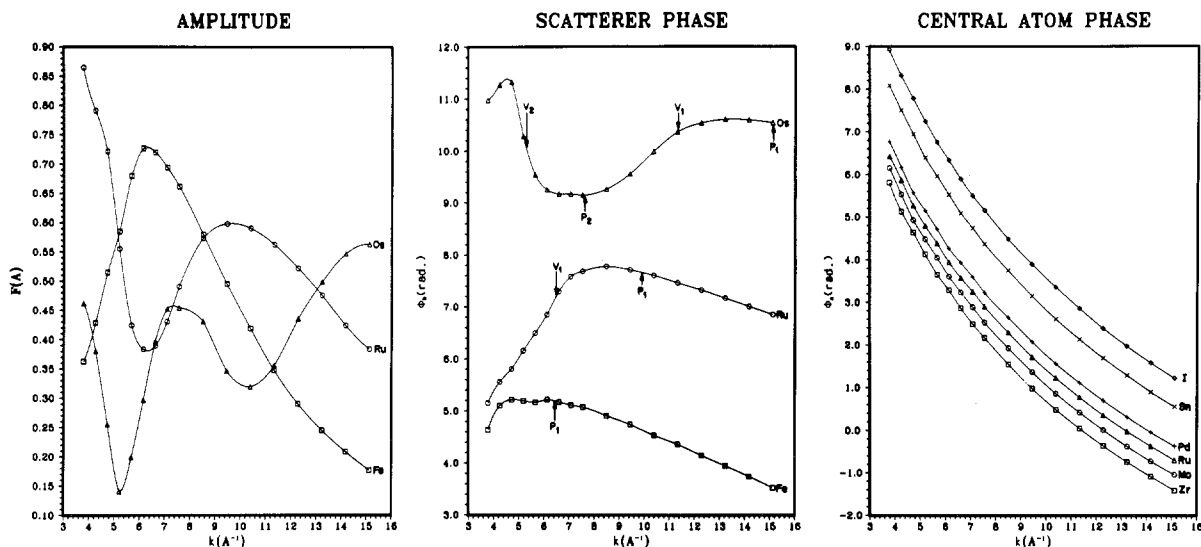
Figure 3. Theoretical backscattering amplitude (left), backscattering phase (middle), and central atom (absorber) phase (right) functions for some elements.
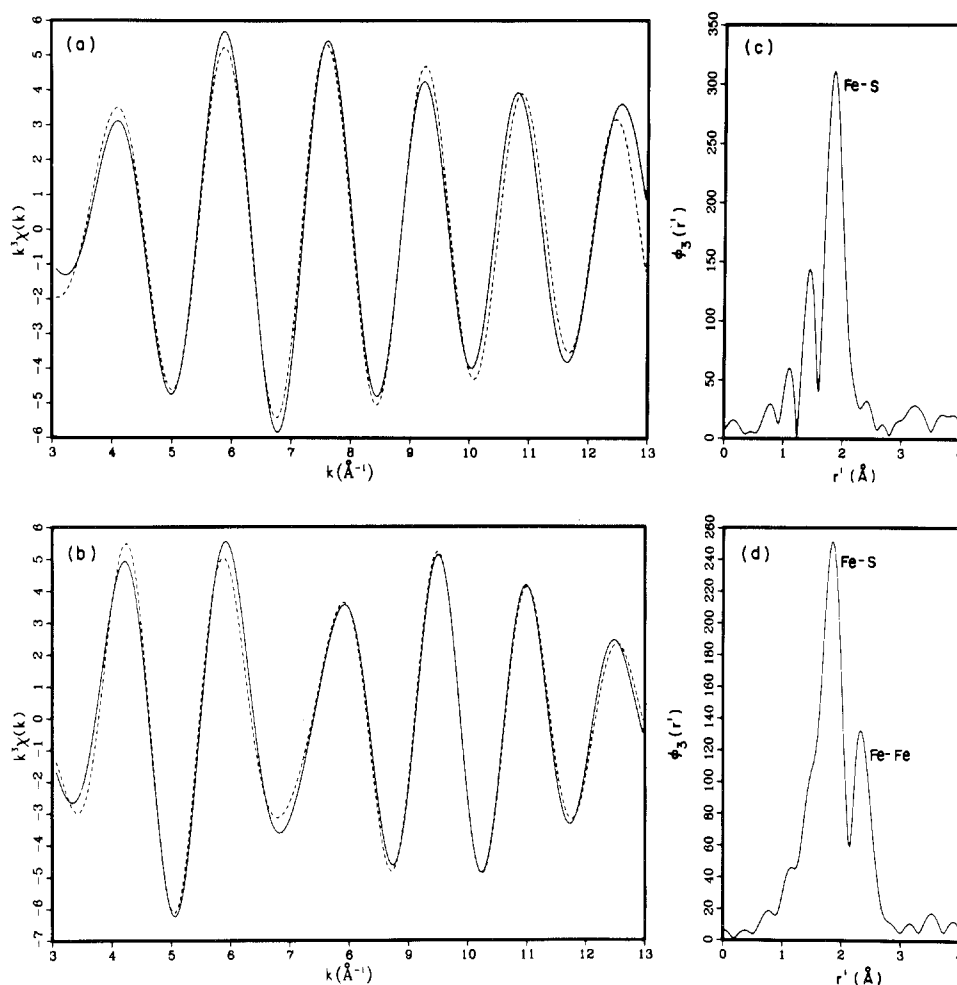

Figure 4. Fourier filtered (window: $r' = 0.9 \sim 3.5$ Å) EXAFS spectra (solid curves) and the theoretical fits (dashed curves) for (a) *single-shell* systems such as rubredoxin and (b) *two-shell* systems such as bacteria ferredoxin. In (a) a single term containing the average Fe–S distance was used whereas in (b) two terms containing the average Fe–S and Fe–Fe distances were used. The corresponding Fourier transforms of the $k^3\chi(k)$ vs. k data are shown in (c) and (d), respectively. The minor peaks to the left of the Fe–S peak are due to residual background and/or Fourier truncation.

tion or assessment of steric vs. electronic effects of the active site. This is exemplified by our EXAFS studies of iron–sulfur proteins.[16] It is known that there are

four prototypes of non-heme iron–sulfur proteins containing one, two, four, or eight iron atoms. The minimal prosthetic groups are $Fe(SR)_4$ in rubredoxin, $Fe_2S_2(SR)_4$ in plant ferredoxins (Fd), and $Fe_4S_4(SR)_4$ in 'high-potential' iron proteins (HIPIP) and bacterial ferredoxins.

(16) For an excellent review, see R. H. Holm, *Acc. Chem. Res.* **10**, 427 (1977).

Iron EXAFS of these proteins are dominated by neighboring sulfur and iron atoms of the active sites.[17,18] The amplitude envelope of the monomeric $Fe(SR)_4$ species varies smoothly with **k** (cf. Figure 4a), indicative of a single-shell system with one type of distance. In contrast, the amplitude envelope of the diiron and tetrairon oligomers exhibits a "beat" node at **k** ≈ 7 Å^{-1} which is characteristic of two-shell systems with two types of distances (cf. Figure 4b). The frequency at lower **k** region, which reflects the shorter Fe–S bonds, is lower than the frequency at higher **k** region, which is indicative of the longer Fe–Fe bonds. Fourier transforms of the $\chi(k)k^3$ data reveal in both solid and solution states only one peak for the monomer (cf. Figure 4c) but two peaks for the two oligomers (cf. Figure 4d). The major peak can be assigned to the Fe–S bonds while the minor peak in each of the oligomers can be assigned to the Fe–Fe bonds.[17,18]

In most applications, EXAFS provides only the average distances. Nevertheless, the Debye–Waller factor can indicate the spread of the distances. For example, from the experimentally determined σ_{stat}, it was concluded that the Fe–S bonds in rubredoxin are chemically equivalent to within 0.04 Å,[17] in contrast to the original crystallographic finding.[19]

EXAFS provides an excellent opportunity for correlating structural parameters with redox states of the proteins, both in the *solid state* and in *solution*. For example, the average Fe–S distance in rubredoxin was found to lengthen by 0.06 Å upon reduction[17] whereas the lengthening of Fe–S and Fe–Fe bonds in the oligomers upon reduction was quite small (viz., ≤ 0.03 Å).[18] Furthermore, little change (within 0.02 Å) was found in the average structural parameters upon dissolution of the proteins.[18]

EXAFS has also been used to probe the stereochemical nature of a variety of metal-containing biopolymers. For the presumably relaxed porphyrin rings in deoxyhemoglobins, the iron atom was found to be only 0.2 Å (with a limit of +0.1 or −0.2 Å) out of the plane.[20a,b] This is significantly less than the 0.75-Å displacement of the iron atom from the mean porphyrin plane as suggested by the Hoard–Perutz model.[20c,d] EXAFS studies[21] on carbonic anhydrase, an enzyme which catalyzes the reaction $H_2O + CO_2 \rightleftarrows H_2CO_3$, and on its iodide complex provide evidence that the iodide, an anionic inhibitor, is directly coordinated to the zinc atom at a normal covalent Zn–I distance of 2.65 (6) Å. This should be contrasted with the crystallographic finding that the iodide ion lies between 3.5 and 3.7 Å from the zinc atom. An elegant study[22] on the iron-storage protein ferritin indicated that each of the iron atoms in the micellar core is surrounded by 6.4 (6) oxygens at 1.95 (2) Å (probably in a distorted octahedral
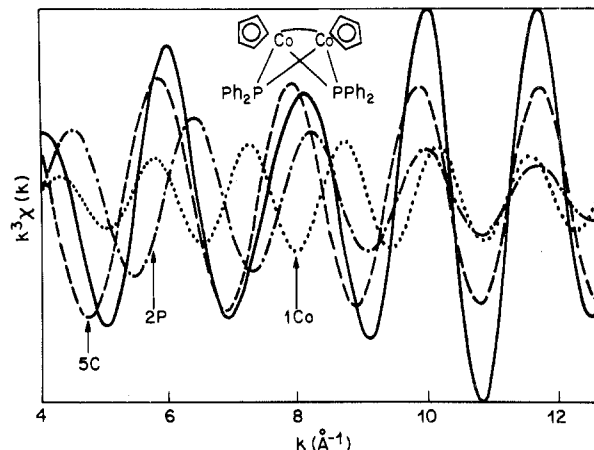

Figure 5. A *three-shell* system: the filtered EXAFS spectrum (—) of $[CpCoPPh_2]_2$ is resolved into three backscattering components by curve fitting: 5C (- - -), 2P (-----), 1 Co (···). The fitting model involves a sum of three terms which arise from five Co–C bonds, two Co–P bonds, and one Co–Co bond surrounding each cobalt atom. Each term contains the corresponding average distance and the Debye-Waller factor which are least-squares refined. The ordinate scales are −5.93 to 5.33 Å^{-3}.

arrangement) with 7 (1) neighboring iron atoms at 3.29 (5) Å. A layered, strip structure, in which the iron atoms are in the interstices between two nearly close-packed layers of oxygens with approximate sixfold rotational symmetry, was proposed. These authors[22] believe that the ferritin core is formed by a folding of one such strip back and forth upon itself in the form of a pleat. From a recent EXAFS study[23a] of the molybdenum site in the enzyme nitrogenase, it was concluded that the Mo atom is bonded to 3.8 sulfur atoms at 2.35 Å, 3.0 iron atoms at 2.72 Å, and 1–2 sulfur atoms at ~ 2.55 Å. These findings are consistent with a cubane-like $MoFe_3S_4$ cluster model previously proposed for the Mo site.[23b] A different interpretation, however, led to a new structural model for the enzyme.[23c] A recent EXAFS study on oxy- and deoxyhemocyanin (Hc) led to a model of the Hc binding site as having two Cu atoms bound to the protein via three histidine ligands. In oxyHc the Cu(II) ions are bridged by the bound O_2^{2-} and another ligand, possibly tyrosine.[23d] Other EXAFS applications in biochemistry and related disciplines can be found in SSRL Reports.[24]

Another important application of EXAFS spectroscopy is to provide information about local structures of drugs before and after their interactions with biological systems. In fact, it may ultimately be possible to study drug actions on living organisms such as intact cells, in vitro or in vivo. Since EXAFS can focus on the absorbing atoms (usually the heavy atoms), no separation or isolation is required. In this context, we note that several importnt antitumor platinum drugs and their interactions with DNA have been studied by EXAFS.[25]

(17) R. G. Shulman, P. Eisenberger, B. K. Teo, B. M. Kincaid, and G. S. Brown, *J. Mol. Biol.*, **124**, 305 (1978), and references cited therein.

(18) B. K. Teo, R. G. Shulman, G. S. Brown, and A. E. Meixner, *J. Am. Chem. Soc.*, **101**, 5624 (1979).

(19) K. D. Watenbaugh, L. C. Sieker, J. R. Herriot, and L. H. Jensen, *Acta Crystallogr., Sect. B*, **29**, 943 (1973).

(20) (a) P. Eisenberger, R. G. Shulman, G. S. Brown, S. Ogawa, *Proc. Natl. Acad. Sci. U.S.A.*, **73**, 491 (1976); (b) P. Eisenberger, R. G. Shulman, B. M. Kincaid, G. S. Brown, and S. Ogawa, *Nature (London)*, **274**, 30 (1978); (c) J. L. Hoard, *Science*, **174**, 1295 (1971); (d) M. F. Perutz, *Nature (London)*, **228**, 726 (1970).

(21) G. S. Brown, G. Navon, and R. G. Shulman. *Proc. Natl. Acad. Sci. U.S.A.*, **74**, 1794 (1977).

(22) S. M. Heald, E. A. Stern, B. Bunker, E. M. Holt, and S. L. Holt, *J. Am. Chem. Soc.*, **101**, 67 (1979).

(23) (a) T. E. Wolff, J. M. Berg, C. Warrick, K. O. Hodgson, R. H. Holm, and R. B. Frankel, *J. Am. Chem. Soc.*, **100**, 4630 (1978); (b) S. P. Cramer, K. O. Hodgson, W. O. Gillum, and L. E. Mortenson, ibid, **100**, 3398 (1978); (c) B. K. Teo and B. A. Averill, *Biochem. Biophys. Res. Commun.*, **88**, 1454 (1979); (d) J. M. Brown, L. Powers, B. Kincaid, J. A. Larrabee, and T. G. Spiro, *J. Am. Chem. Soc.*, **102**, 4210 (1980).

(24) For example, SSRL Publication List; SSRL Reports 78/10, 79/03, 79/10, 80/01, etc.

(25) (a) B. K. Teo, K. Kijima, and R. Bau, *J. Am. Chem. Soc.*, **100**, 621 (1978), and references cited therein; (b) B. K. Teo, P. Eisenberger, J. Reed, J. K. Barton, S. J. Lippard, *ibid.*, **100**, 3225 (1978), and references cited therein.

Inorganic and Catalytic Systems

EXAFS is useful in inorganic chemistry, especially when single crystals are not available or when structural information in solution is sought. It is capable of differentiating between metal–metal and metal–ligand bonds provided that the atomic numbers of the neighboring metal and ligand atoms are sufficiently different ($\Delta Z \gtrsim 4$).[13]

EXAFS study of the chemically unstable, "one-electron" metal–metal bonded cobalt cluster $[CpCoPPh_2]_2^+$ ($Cp = \eta^5\text{-}C_5H_5$; $Ph = C_6H_5$) provided the first structural evidence that the metal–metal bond is significantly weakened upon oxidation of the neutral dimer to the monocation.[26] The neutral dimer (inset of Figure 5) was crystallographically shown to possess a bent Co_2P_2 core of C_{2v} geometry with an electron-pair Co–Co bond of 2.56 (1) Å. Its EXAFS spectrum is shown in Figure 5 (solid curve) along with the three backscattering components (5C + 2P + 1Co), which were resolved by curve fitting.[26] For the monocation, the magnitude of the cobalt backscatteing (1Co) decreases significantly. On the basis of a difference Fourier technique, a small increase in the Co–Co distance of 0.08 Å (from 2.57 (1) to 2.65 (5) Å) and a significant weakening of the Co–Co bond, as indicated by a significant increase in the Debye–Waller factor (from 0.058 (4) to 0.10 (2) Å), are observed in going from the neutral parent to the monocation.

Other EXAFS applications involving inorganic systems[24,27–31] include iron and molybdenum complexes,[27] metallic glasses,[28] superconductors,[29a] superionic conductors,[29b] semiconductors,[29c] solutions,[30a–c] molten salts,[30d,e] and liquid metals.[31]

Another important use of EXAFS is the determination of local structures of the catalytic sites of homogeneous or heterogeneous catalysts (supported or unsupported),[32,33] In a study of the structural variation of the catalytic site of the polymer-bound bromo-Wil-

kinson's catalyst ($Rh(PPh_3)_3Br$) as a function of the degree of cross-linking,[32a] the K edges of both rhodium and bromine atoms were measured. For the Rh EXAFS, the characteristic multidistance interference pattern (with a beat node at $\mathbf{k} \approx 9$ Å^{-1}) required a two-shell, three-distance model ($Rh–P_1$, $Rh–P_2$, and $Rh–Br$) for curve fitting whereas for the Br EXAFS, a single-shell model (Br–Rh) was adequate. These results suggested a dibromo-bridged dirhodium species ($P_2RhBr_2RhP_2$) for 2% cross-linking but a monomeric species (RhP_3Br) for 20% cross-linking[32a] of the polymer.

Sinfelt, Lytle, and others[24,33] have studied a large number of supported metal catalysts by EXAFS which have provided a better understanding of their structures. The general conclusions are as follows.[24,33] With cluster size $\gtrsim 15$ Å, the metal–metal distances and the coordination numbers are similar to those of the bulk metal. As the metal dispersion (viz., the surface-to-total atom ratio) increases, the metal cluster size becomes smaller which results in a small decrease ($\lesssim 0.03$ Å) in the metal–metal distance, a large decrease in the coordination number (from 12 in the bulk to 7–10), and a significant increase in the Debye–Waller factor (by a factor of 1.4–2) for the first shell. Relative to the first shell, the higher shells also lose peak magnitudes but at a faster rate. These observations suggest a raft-like structure for the highly dispersed clusters. In addition, peaks due to metal–support interactions may also be observed with increasing metal dispersion.[24,33] Most recently, studies on supported bimetallic catalysts such as silica-supported Ru–Cu indicated that the bimetallic clusters contain a ruthenium-rich core and a copper-rich surface.[33e]

EXAFS: Strength, Weakness, and Its Future

There are several highly attractive features of the EXAFS technique which makes it a powerful structural tool. First, it is extremely fast. With synchrotron radiation, each spectrum per element takes 10–15 min, though for dilute systems, data averaging or specialized instrumentation may be required. With laser-produced X-rays, a spectrum can be recorded on film in a few nanoseconds. Second, both sample preparation and data collection are relatively easy. No single crystals are required. Third, being sensitive to short-range order in atomic arrangements rather than long-range crystalline order, EXAFS can focus on the local environment of specific absorbing atoms. Fourth, the EXAFS technique can be used for a wide variety of materials such as amorphous solids, liquids, solutions, gases, polymers, and surfaces.

An obvious deficiency of EXAFS spectroscopy lies in the fact that it does not provide full three-dimensional structural details. It gives only local structures in terms of one-dimensional radial distribution functions about each absorber. The absorbing atoms are preferably different in atomic number or equivalent in chemical environment. Any absorbing element appearing in several different chemical states (or environments) will greatly complicate the interpretation of its EXAFS data which is a superpositon of all the states. No *direct* method of determining angular information is available

(26) B. K. Teo, P. Eisenberger, and B. M. Kincaid, *J. Am. Chem. Soc.*, **100**, 1735 (1978).

(27) (a) S. P. Cramer, T. K. Eccles, F. Kutzler, K. O. Hodgson, and S. Doniach, *J. Am. Chem. Soc.*, **98**, 8059 (1976); (b) S. P. Cramer and K. O. Hodgson, *ibid.*, **100**, 2748 (1978).

(28) (a) H. S. Chen, B. K. Teo, and R. Wang, *Abstr. 4th Int. Conf. Liq. Amor. Metals*, Grenoble, France, July 7–11, 1980; (b) J. Wong, F. W. Lytle, R. B. Greegor, H. H. Liebermann, J. L. Walter, and F. E. Luborsky, *Proc. 3rd Inter. Conf. Rapid. Quench. Metals*, Sessex University, Vol. II, 1978, p 1345; (c) T. M. Hayes, J. W. Allen, J. Tauc, B. C. Giessen, and J. J. Hauser, *Phys. Rev. Lett.*, **40**, 1282 (1978); (d) E. A. Stern, S. Rinaldi, E. Callen, S. Heald, and B. Bunker, *J. Magn. Mater.*, **7**, 188 (1978).

(29) (a) G. S. Brown, L. R. Testardi, J. H. Wernick, A. B. Hallak, and T. H. Geballe, *Solid State Commun.*, **23**, 875 (1977); (b) J. B. Boyce and T. M. Hayes, *Top. Curr. Phys.*, **15**, Chapter 2 (1979); (c) S. Hunter, A. Bienenstock, and T. M. Hayes, in "Structure of Non-Crystalline Materials", P. H. Gaskell, Ed., Taylor and Francis, London, 1977, p 73; S. H. Hunter, A. Bienenstock, and T. M. Hayes in"Amorphous and Liquid Semiconductors", W. E. Spear, Ed., University of Edinburgh, Edinburgh, 1977, p 78.

(30) (a) P. Eisenberger and B. M. Kincaid, *Chem. Phys. Lett.*, **36**, 134 (1975); (b) D. R. Sandstrom, H. W. Dodgen, and F. W. Lytle, *J. Chem. Phys.*, **67**, 473 (1977); (c) D. R. Sandstrom, *ibid.*, **71**, 2381 (1979); (d) E. D. Crozier, F. W. Lytle, D. E. Sayers, and E. A. Stern, *Can. J. Chem.*, **55**, 1968 (1977); (e) J. Wong and F. W. Lytle, *J. Non-Cryst. Solid.*, **37**, 273 (1980).

(31) E. D. Crozier and A. J. Seary, *Can. J. Phys.*, **58**, 1388 (1980).

(32) (a) J. Reed, P. Eisenberger, B. K. Teo, and B. M. Kincaid, *J. Am. Chem. Soc.*, **100**, 2375 (1978); (b) J. Reed, P. Eisenberger, B. K. Teo, and B. M. Kincaid, *ibid.*, **99**, 5217 (1977).

(33) (a) J. H. Sinfelt, G. H. Via, and F. W. Lytle, *J. Chem. Phys.*, **68**, 2009 (1978); (b) F. W. Lytle, *NBS Spec. Publ. (U.S.)*, **475**, 34 (1977); (c) I. Bassi, F. W. Lytle, and G. Parravano, *J. Catal.*, **42**, 139 (1976); (d) G. H. Via, J. H. Sinfelt, and F. W. Lytle, *J. Chem. Phys.*, **71**, 690 (1979); (e) J. H. Sinfelt, G. H. Via, and F. W. Lytle, *J. Chem. Phys.*, **72**, 4832 (1980); (f) ref 6c.

(34) (a) S. M. Heald and E. A. Stern, *Phys. Rev. B*, **16**, 5549 (1977); (b) L. I. Johansson and J. Stohr, *Phys. Rev. Lett.*, **43**, 1882 (1979).

(except from single-crystal measurements utilizing polarized X-rays[34]). Furthermore, EXAFS diminishes rapidly beyond the first and second coordination shells (typically $r \lesssim 4$ Å) except in cases where atoms are nearly collinear. In such cases, EXAFS from atoms as far as 6 Å can be observed due to amplitude enhancement called focusing effect. In fact, both amplitude and phase of the EXAFS of a more distant neighbor are significantly affected by the intervening atom(s) for bond angle > 120°. For these systems, one must therefore take into account multiple scattering processes involving the intervening atom(s). Recently, a new multiple scattering formalism has been developed[35] which enables bond angle determinations with an accuracy of 5% or ca. 5°.

Nevertheless, the structural content of EXAFS is unparalleled by other spectroscopic techniques when

one considers that the few most important bonds in a complex system can be probed within minutes. The future of EXAFS spectroscopy is as bright as the future synchrotron radiation sources. Dedicated synchrotron radiations with energy ranging from UV to hard X-rays are now available.[36] These highly intense light sources will undoubtedly open up a new era in exciting chemical, biological, and material research.

(35) B. K. Teo, submitted for publication.

(36) Four major facilities are being planned in the United States: an expanded SSRL at Stanford, CHESS at Cornell, Aladdin at Wisconsin, and National Synchrotron Light Source at Brookhaven National Laboratory.

Mechanism of the Ene Reaction between Singlet Oxygen and Olefins

L. M. Stephenson*

Department of Chemistry and Hydrocarbon Research Institute, University of Southern California, Los Angeles, California 90007

Mary Jo Grdina and Michael Orfanopoulos

Department of Chemistry, Case Western Reserve University, Cleveland, Ohio 44107

Received December 21, 1979 (Revised Manuscript Received August 15, 1980)

Singlet molecular oxygen has been studied since the 1930s,[1] and photosensitized oxygenations of olefins have been synthetically useful for some time.[2] Representative examples of these transformations are given in eq 1–3.[3]
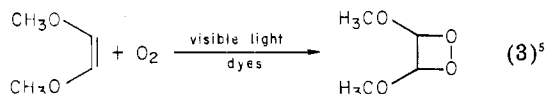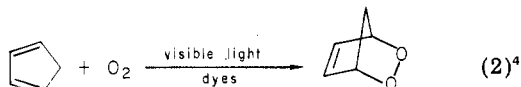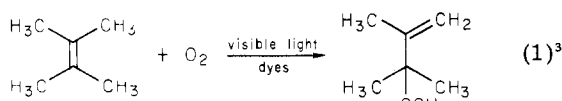
In the last 40 years these reactions have been extensively studied both to determine synthetic utility[6] and to elucidate mechanisms.[6b,7] These oxygenations represent one of the most important hydrocarbon functionalization reactions available to the synthetic organic chemist. This chemistry has also been related both speculatively and rigorously to such diverse areas as air pollution,[8] photocarcinogenicity,[9] and chemiluminescence.[10] Remarkably, however, no agreement exists either informally or in the literature on the mechanisms of these transformations.

It would be difficult to find a more appropriate vehicle for illustrating reaction mechanism methodology than photosensitized oxygenation; virtually every mechanistic technique has been applied to the study of these reactions. The identification of the reactive intermediate in these systems involved spectral tests,[11]

L. M. Stephenson is a native of North Carolina and a graduate of the University of North Carolina at Chapel Hill. Following graduate work at Caltech and a postdoctoral year at Harvard, he embarked on a nomadic career which includes stops at Stanford and Case Western Reserve University. He is presently Professor of Chemistry and Director of the Hydrocarbon Research Institute at USC.

Mary Jo Grdina was born and educated in Cleveland. She received a bachelor's degree from Notre Dame College of Ohio, and a doctorate from Case Western Reserve University in 1979. She taught for a number of years at Notre Dame College, and recently joined the faculty at Oberlin College.

Michael G. Orfanopoulos was born in Athens, Greece. He received his bachelor's degree from the University of Patras, followed by an M.S. from Toledo and a Ph.D. from Case Western Reserve University in 1979. He is presently a postdoctoral fellow at Stanford.

(1) Childs, W. H. J.; Mecke, R. Z. *Physik* 1974, *68*, 334.
(2) Schenck, G. O. German Patent 933 925, 1943.
(3) Schenck, G. O.; Schulte-Elte, K. *Liebigs Ann. Chem.*, 1958, *618*, 185.
(4) Schenck, G. O.; Ziegler, K. *Naturwissenschaften* 1945, *32*, 157.
(5) Bartlett, P. D.; Schaap, A. P. *J. Am. Chem. Soc.* 1970, *92*, 3223, 6055.
(6) (a) Denny, R. W.; Nickon, A. *Org. React.* 1973, *20*, 133. (b) Gollnick, K.; Kuhn, H. J. In "Singlet Oxygen"; Wasserman, H. H., Murray, R. W., Eds.; Academic Press: New York, 1979, p 287.
(7) (a) Foote, C. S. *Acc. Chem. Res.* 1968, *1*, 104. (b) Ranby, B., Rabek, J. F., Eds. "Singlet Oxygen Reactions with Organic Compounds and Polymers", Wiley: New York, 1978.
(8) Pitts, J. N., Jr., *Ann. N.Y. Acad. Sci.* 1970, *171*, 239.
(9) Khan, A. U.; Kasha, M. *Ann. N.Y. Acad. Sci.* 1970, *171*, 24.
(10) Kearns, D. R. *Chem. Rev.* 1971, *71*, 395, 424.